Disposition of nanoparticles and an associated lipophilic permeant following topical application to the skin

Journal:	*Molecular Pharmaceutics*
Manuscript ID:	mp-2009-001188.R1
Manuscript Type:	Article
Date Submitted by the Author:	
Complete List of Authors:	Wu, Xiao; University of Bath, Pharmacy & Pharmacology Price, Gareth; University of Bath, Department of Chemistry Guy, Richard; University of Bath, Pharmacy & Pharmacology

Disposition of Nanoparticles and an Associated Lipophilic Permeant following Topical Application to the Skin

Xiao Wu[1], Gareth J. Price[2] and Richard H. Guy[1,*]

[1]*Department of Pharmacy and Pharmacology, University of Bath, Claverton Down, Bath, BA2 7AY, U.K.*

[2]*Department of Chemistry, University of Bath, Claverton Down, Bath, BA2 7AY, U.K.*

Running title: Disposition of Polymeric Nanoparticles on Skin

[*] To whom correspondence should be addressed. R.H.G.: Department of Pharmacy and Pharmacology, University of Bath, Claverton Down, Bath, BA2 7AY, U.K.; phone, +44.1225.384901; fax, +44.1225.386114; e-mail, r.h.guy@bath.ac.uk.

For Table of Contents Use Only

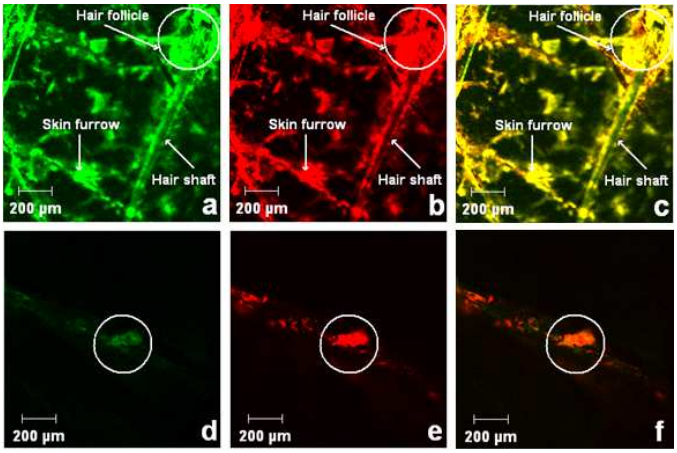

Manuscript title: Disposition of Nanoparticles and an Associated Lipophilic Permeant following Topical Application to the Skin

Authors: Xiao Wu, Gareth J. Price and Richard H. Guy

Abstract: The objective was to determine the disposition of polymer nanoparticles and an associated, lipophilic, model "active" component on and within the skin following topical application. Polystyrene and poly(methyl methacrylate) nanoparticles containing covalently bound fluorescein methacrylate and dispersed Nile Red were prepared by emulsion polymerization. The two fluorophores differentiate the fate of the polymeric vehicle on and within the skin from that of the active. Nanoparticles were characterized by dynamic light scattering, transmission electron microscopy and NMR spectroscopy. In-vitro skin permeation experiments were performed using dermatomed porcine skin. Post-treatment with nanoparticle formulations, the skin surface was either cleaned carefully with buffer, or simply dried with tissue, and then immediately visualized by confocal microscopy. Average nanoparticle diameters were below 100 nm. Confocal images showed that nanoparticles were located in skin "furrows" and around hair follicles. Surface cleaning removed the former but not all of the latter. At the skin surface, Nile Red remained partly associated with nanoparticles, but was also released to some extent and penetrated into deeper layers of the stratum corneum (SC). In summary, polymeric nanoparticles did not penetrate beyond the superficial SC, showed some affinity for hair follicles, and released an associated "active" into the skin.

Keywords: Nanoparticles; skin; laser scanning confocal microscopy (LSCM); topical drug delivery.

Introduction

Recently, polymeric nanoparticles (NP) have been proposed as carriers for drugs and other active agents administered by topical administration. Examples include anti-inflammatory drugs,[1, 2] anti-infective drugs, vitamins[3] and sunscreens.[4-6] It has been claimed that drug-loaded NP achieve sustained release and consequently improve the therapeutic effect of dermatological formulations.[2, 3] More importantly, NP can increase the stability of sensitive actives by protecting the molecules in a polymeric shell. Based on this, NP have been incorporated into several commercially available cosmetic products to encapsulate various actives (e.g., vitamin A, rose extract and wheat germ oil).

The development of topical formulations containing nano-sized materials has also been challenged by mechanistic and toxicity issues. Compared with larger particles, it has been suggested that nanostructures are more likely to penetrate the stratum corneum and gain access to the living cells within the epidermis and dermis. Should this be possible, then systemic exposure might occur (i.e., the nanoparticles being taken up into the blood and distributed to various tissues and organs), presenting thereby a potential toxicity risk for human health.[7-10] Therefore, understanding the topical disposition of both vehicle and active is essential for the use of nano-engineered topical formulations. Whether (and when) the active is released from the vehicle, and the fate of the vehicle itself, are very important questions concerning the safety of nanotechnology. To address these issues, two series of polymeric NP have been prepared in which the polymer was covalently-labelled with fluorescein methacrylate (FMA, Chart 1a). A second fluorescent compound, Nile Red (NR, Chart 1b) was incorporated into the particles to simulate a hydrophobic active. Laser scanning confocal microscopy (LSCM) was used to track both fluorophores after topical application to porcine skin.

Porcine skin is a good substitute for human skin having epidermal thickness, lipid composition, permeability, transepidermal water loss and low frequency impedance values which are very similar.[11, 12]

Chart 1. Chemical structures of fluorescein methacrylate (FMA) and Nile Red (NR).

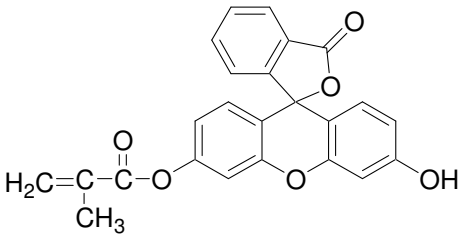

(a) FMA

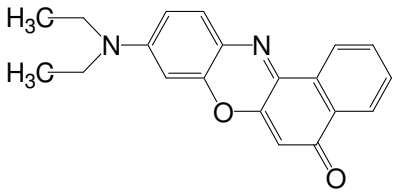

(b) NR

Materials and Methods

Tissue. Full thickness porcine skin was obtained from a local slaughterhouse. The skin was cleaned carefully under cold running water. The subcutaneous fat was removed with a scalpel. The remaining tissue was dermatomed to a thickness of ~750 µm. Finally, the dermatomed skin was stored frozen at -20°C for up to a maximum of one month before use.

Chemicals. Fluorescein O-Methacrylate (97% pure), Nile Red (analytical grade) and polystyrene (PS, MW: 44,000) were purchased from Sigma-Aldrich (St. Louis, MO, USA). Styrene (99% GC), methyl methacrylate (MMA, 99% GC) and potassium persulfate (KPS) were purchased from Sigma-Aldrich (Gillingham, Dorset, England). Other chemicals used were polymethylmethacrylate (PMMA, MW = 50,000 Fluka Analytical, Steinhelm, Germany), sodium

dodecylsulphate (SDS, 99+% GC, Sigma-Aldrich, Japan), ruthenium tetroxide (Taab Laboratories, Aldermaston, England), phosphotungstic acid (Agar Scientific Ltd., Stansted, UK), and chloroform-d_1 (ISOTEC TM, Miamisburg, OH, USA).

Nanoparticle (NP) Preparation. Before use, inhibitors were removed from the vinyl monomers by passage through an alumina column. The NP were prepared in an inert nitrogen atmosphere by free radical polymerization (see Scheme 1).

Scheme 1. Polymerization of styrene (Reaction A) and methyl methacrylate (MMA) (Reaction B) with fluorescein methacrylate (FMA) using potassium persulfate (KPS) as an initiator at 75℃.

Reaction A:

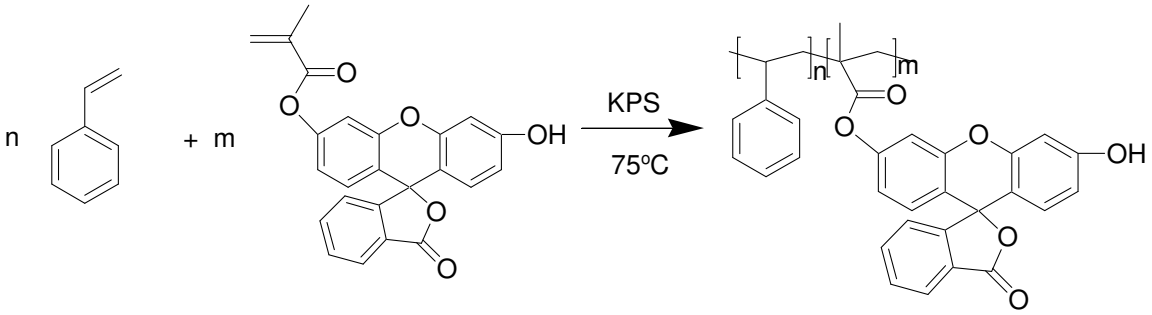

Styrene FMA FMA-Polystyrene

Reaction B:

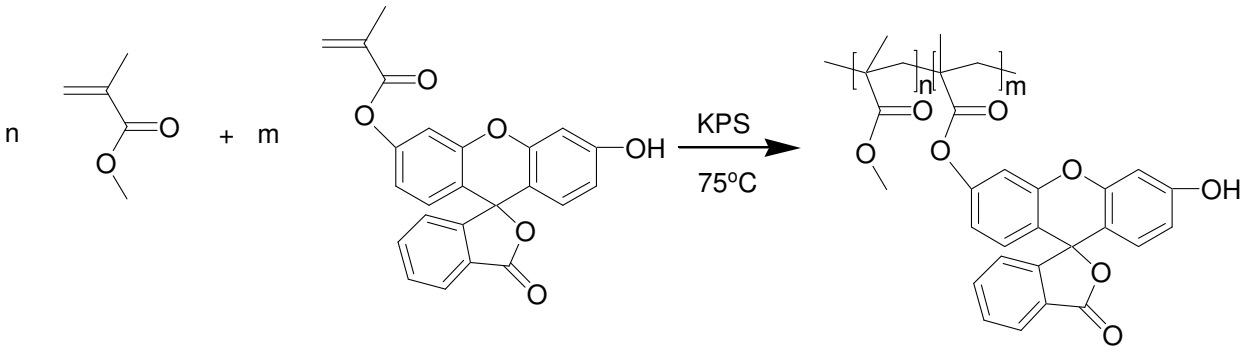

MMA FMA FMA-PMMA

200 cm^3 distilled water was placed in a round bottom flask, with 1 g of SDS added as an emulsifier. The aqueous surfactant solution was deoxygenated with N_2. 13 g of deoxygenated styrene was added into the aqueous phase. The mixture was vigorously stirred to form an emulsion and heated to 75°C. To start the polymerization, 0.1 g KPS dissolved in a small amount of water was added. The reaction was allowed to proceed under nitrogen for 3 hours. To prepare fluorescently labeled NP, 0.13 g of FMA and/or 0.13 g NR were mixed with the monomer before addition to the reaction. The same procedure was used for the preparation of PMMA NP.

NP Characterization. The mean size and polydispersity of the NP were measured with dynamic light scattering (DLS BI90Plus, Brookhaven Instruments Corporation, NY, USA). The morphology of the nanoparticles was observed on a JEOL JEM-2000 transmission electron microscope (TEM) at an accelerating voltage of 120kV. Each sample was prepared by casting a drop of NP dispersion onto a 300-mesh copper grid covered with carbon film. TEM images of PS NP were obtained as positively stained preparations by placing samples in ruthenium tetroxide vapour for 1 hour. TEM images of PMMA NP were obtained as negatively stained preparations by placing samples in phosphotungstic acid for 1 hour. ^1H NMR spectra were recorded in deuterated chloroform ($CDCl_3$) on a Bruker Avance™ III spectrometer (Billerica, MA, USA) operating at 400 MHz. Prior to analysis, the NP were washed with water and acetone to remove SDS and unreacted compounds, and freeze-dried (Heto PowerDry PL3000, Thermo Electron corporation, Waltham, MA, USA).

***In vitro* Skin Permeation.** Before the experiment, the hairs were trimmed as close as possible to

the skin surface. Skin permeation experiments were performed in vertical Franz diffusion cells thermostated at 37°C. The excised tissue was clamped between the donor and receptor compartments exposing a diffusion area of 3.8 cm^2. The receptor compartment was filled with physiological buffer (pH = 7.4); the donor compartment held 1 cm^3 of the NP formulation and was covered with Parafilm. After 6 hours of exposure, the cell was dismantled, and the skin surface was either cleaned carefully with physiological buffer or was simply patted dry with tissue and then immediately visualized by confocal microscopy.

Laser Scanning Confocal Microscopy (LSCM). The skin was examined using a LSM 510 Invert Laser Scanning Microscope (Carl Zeiss, Jena, Germany). The system was equipped with an argon laser (excitation line at 488 nm) and a HeNe laser (excitation line at 543 nm). A Plan-Neofluar 10×/0.3 objective, an EC Plan-Neofluar 40×/1.30 oil DIC M27 objective and a Plan-Apochromat 63×/1.40 oil DIC M27 objective were used. Confocal images were obtained in the plane parallel to the sample surface (xy-mode), or in the plane perpendicular (optical sectioning z-stack mode).

Results

NP Characterization. Table 1 summarizes the properties of the NP formulations used in the *in vitro* permeation experiments.

Table 1. Properties of the PS and PMMA nanoparticulate (NP) formulations examined[a]

NP Formulation	Dyes included	Mean size (nm)	PI[b]
PS	None	28.8	0.135
PS-FMA	FMA	28.0	0.141
PS-FMA-NR	FMA and NR	30.9	0.118
PMMA	None	79.0	0.171
PMMA-FMA	FMA	99.9	0.163
PMMA-FMA-NR	FMA and NR	68.5	0.133

[a] PS = polystyrene; PMMA = polymethylmethacrylate; FMA = fluorescein methacrylate; NR = Nile Red.

[b] PI: polydispersity index of the size distribution (expressed using a 0-1 scale).

The NP were spherical and smooth as shown in Figure 1. The mean diameter of PS NP was less than 50 nm, while the PMMA NP were almost twice as large; these findings were confirmed by dynamic light scattering.

Proton NMR spectra of polystyrene, FMA, PMMA and the two copolymers are shown in Figure 2. Those of the copolymers show signals from either PS or PMMA and FMA even after extensive dissolution/reprecipitation, indicating that FMA is covalently bound to the polymer.

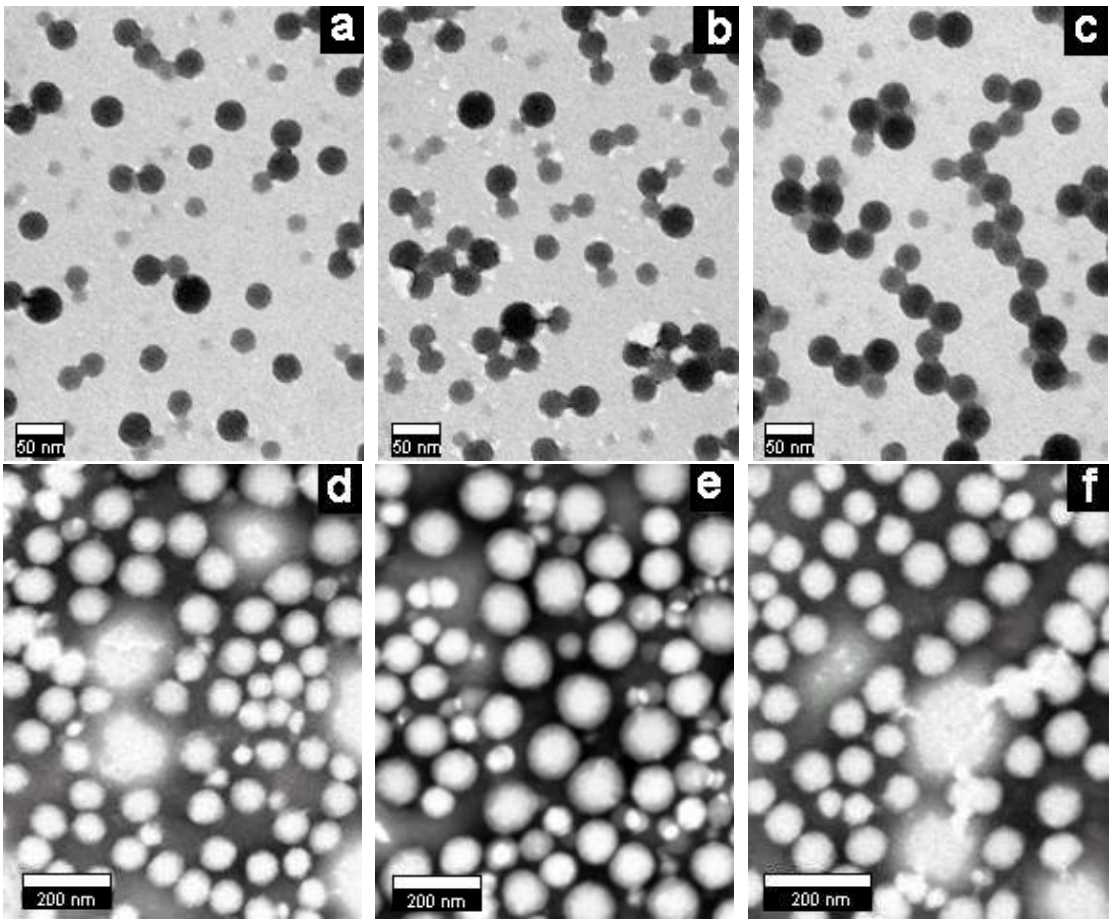

Figure 1. Transmission electron micrograph of PS and PMMA nanoparticles stained with ruthenium tetroxide (a, b and c, scale bar = 50 nm) or phosphotungstic acid (d, e, and f, scale bar = 200 nm). (a) polystyrene NP alone, (b) polystyrene with fluorescein methacrylate (FMA) polymerized, (c) polystyrene with FMA polymerized and Nile Red (NR) absorbed, (d) polymethylmethacrylate (PMMA) NP alone, (e) PMMA with FMA polymerized, and (f) PMMA with FMA polymerized and NR absorbed.

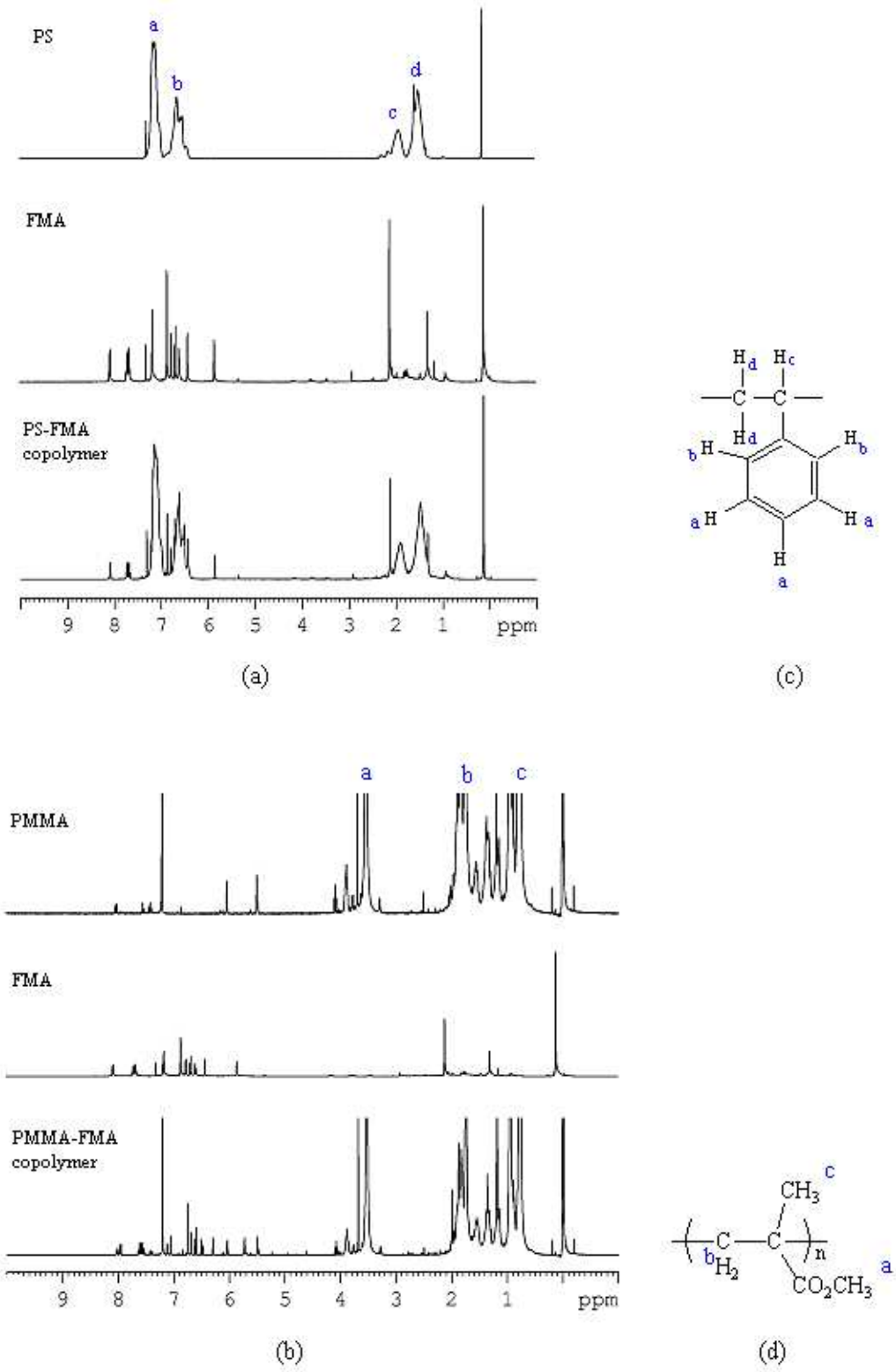

Figure 2. ^{1}H NMR spectra for (a) PS, FMA and PS-FMA copolymer, and (b) PMMA, FMA and PMMA-FMA copolymer, together with the structures and chemical shift assignments of (c) PS, and (d) PMMA.

LSCM Images. Nile Red is commonly used to stain intracellular lipids, because it has an intense and stable red fluorescent emission under the excitation of HeNe laser at 543 nm. It is also a useful model for a topical/transdermal active because of its high lipophilicity (log $P_{o/w} > 3$)[13] and reasonable molecular weight (318.4 $g.mol^{-1}$). FMA is a fluorescent monomer containing a polymerizable methyl acrylate functional group which can react with styrene and MMA. Under excitation at 488 nm, FMA generates a bright green fluorescence, which locates the NP as the dye is covalently bound to polymer. The use of NR and FMA allowed the fate of the NP and of the model lipophilic active to be monitored independently and simultaneously in the same experiment.

Control Experiments. For each formulation, two control experiments were performed to validate the methodology used. Firstly, PS and PMMA nanoparticle formulations without FMA were separately applied to the skin surface. Figures 3a and 3d show the resulting confocal images, which manifest only very weak green fluorescence that is endogenous to the SC. When the fluorescently-labelled NP formulations were applied to the skin, distinctly different LSCM images were observed when the skin was either cleaned properly, or not cleaned at all. Figures 3b and 3e from the latter samples show that the NP were located in the skin furrows and around the hair follicles. In contrast, when the skin was cleaned (Figures 3c and 3f), there was almost no residual fluorescence, suggesting that the NP had remained at the surface and were then easily removed by the simple washing procedure.

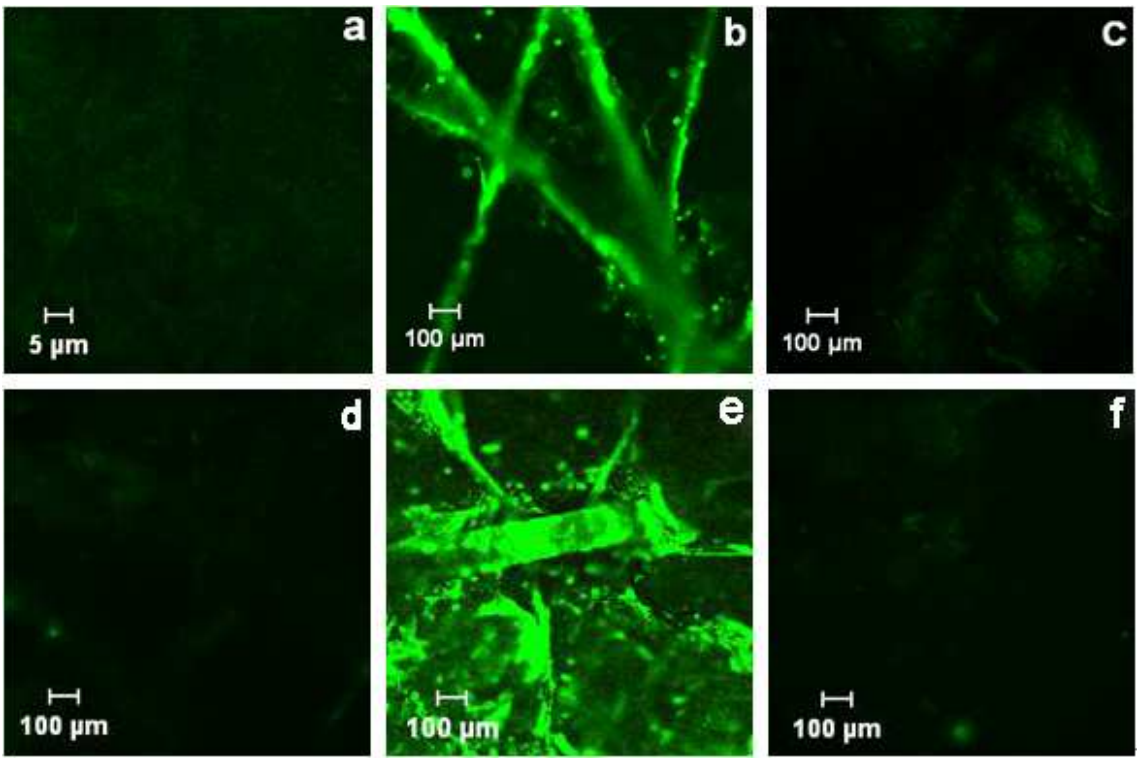

Figure 3. LSCM images of the skin surface following a 6-hour application of PS (panels a, b, c) or PMMA nanoparticles (panels d, e, f). In panels a and d, the NP were not fluorescently labelled with FMA and only a weak green fluorescence from the skin itself is seen. In panels b and e, the NP were fluorescently tagged and the skin surface was not cleaned before imaging; bright green fluorescence is apparent in the skin furrows and around the hair follicles. In panels c and f, the skin surface was cleaned before the confocal images were obtained; only the residual autofluorescence from the skin is observed, suggesting that the NP had been effectively removed by the cleaning procedure.

LSCM Images of Skin Treated with Dual-labelled Fluorescent NP without Surface Cleaning. For skin samples treated with dual fluorophore-labelled NP formulations, LSCM images were acquired using multitracking-mode with excitation wavelengths set at 488nm and 543nm. The fluorescence emission from the two dyes was captured separately and overlaid. Figure 4 and Figure 5 illustrate the disposition of the NP and of Nile Red on and within the skin, the surface of which was not cleaned at the end of the application period, of the polystyrene and polymethylmethacrylate formulations, respectively. Location of the NP is shown by green fluorescence (from FMA

covalently attached to the polymer), while the presence of Nile Red is highlighted in red. For the polystyrene formulation, NP and NR are seen on the skin surface and show clear residence in the skin furrows and around the follicular openings (Figures 4a and 4b). Overlay of green and red fluorescence in Figure 4c clearly emphasizes the co-localization of NP and active.

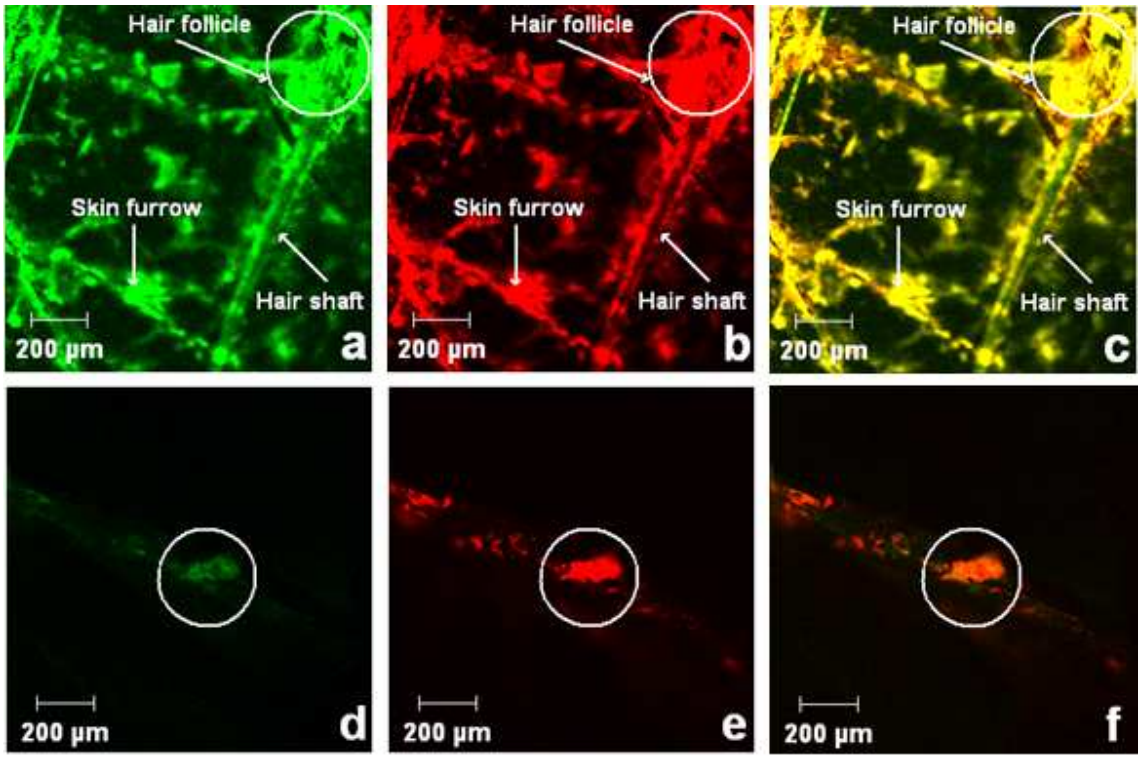

Figure 4. LSCM images (×10) from skin treated with fluorescently-labelled polystyrene NP (31 nm diameter) containing the model active NR. Panels a and b show fluorescence emission from the skin surface from the NP (panel a) and NR (panel b), respectively. Panel c shows the overlay of panels a and b and the co-localization of NP and "active" at the skin surface. Panels d and e illustrate cross-sectional images, respectively highlighting fluorescence from the NP and from NR. A distinctly labelled, short, trimmed hair is visible. Panel f is the overlay of panels d and e and suggests some permeation of released NR to the deeper skin layers.

To examine the fate of the formulation as a function of depth into the skin, the tissue was mechanically sectioned post-treatment and then examined by LSCM at a plane beyond the

mechanical section. The dispositions of NP and NR are shown in Figures 4d and 4e, respectively. Both images highlight a short, trimmed hair shaft on which NP and NR are co-localized. Again, NP are at the surface and NR is seen there too. However, separation of NR from the nanoparticles is apparent (Figure 4f, the overlay) with some permeation of the "active" to the deeper skin layers.

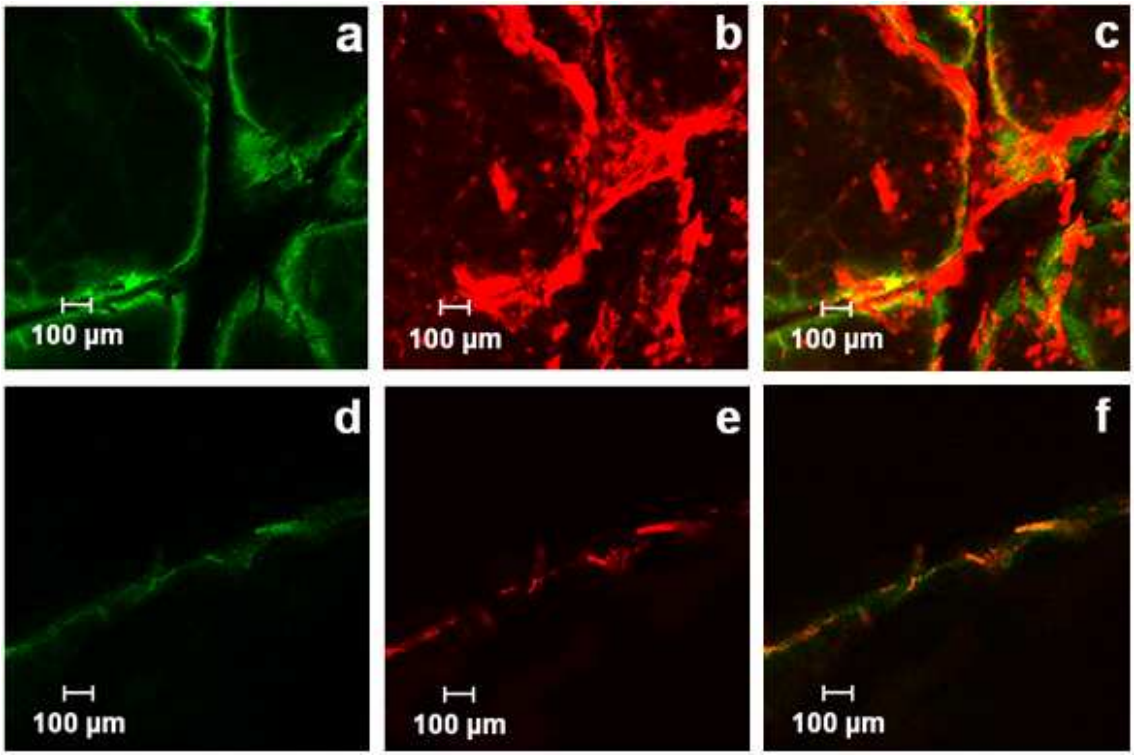

Figure 5. LSCM images (×10) from skin treated with fluorescently labelled polymethylmethacrylate NP (69 nm diameter) containing the model active NR. Panels a and b show fluorescence emission from the skin surface from the NP (panel a) and NR (panel b), respectively. Panel c shows the overlay of panels a and b, the presence of NP in the skin furrows and the release of NR from the NP at the skin surface. Panels d and e illustrate cross-sectional images, respectively highlighting fluorescence from the NP and from NR. Another short hair stub is visibly labelled. Panel f is the overlay of panels d and e and again reveals some degree of separation between NP and NR.

The corresponding images for the polymethylmethacrylate NP containing NR are in Figure 5. Co-localization of the fluorophores in skin furrows (Figures 5a and 5b) is again observed, although

the overlay (Figure 5c) suggests that Nile Red has already been released to some extent at the skin surface. The cross-sectioned images (Figures 5d, 5e and 5f) reveal similar behaviour and again highlight an intensely labelled hair stub.

LSCM Images of Skin Treated with Dual-labelled Fluorescent NP after Surface Cleaning. When the skin surface was properly cleaned by washing with buffer at the end of the 6-hour experiment (as opposed to simply drying off residual solution with a paper tissue), the LSCM images were significantly different. Using the dual-labelled polystyrene NP, post-cleaning there was very little green fluorescence visible (Figure 6a) other than that probably attributable to skin autofluorescence. In contrast, red fluorescence from NR was clearly visible around the corneocytes, presumably reflecting the affinity of the lipophilic "active" for the SC intercellular lipid domains (Figure 6b). Self-evidently, the overlay (Figure 6c) of Figures 6a and 6b reveals only the NR released from the NP prior to their removal by the surface cleaning procedure.

Further examination of the treated skin by optically sectioning the tissue in 1μm steps is shown in Figure 6d. The uptake of NR into the deeper SC is apparent. The appearance of green background autofluorescence can also be seen and demonstrates no greater intensity than that seen in control (untreated) samples, confirming that this signal is not due to the presence of the fluorescently-labelled polymer (data not shown).

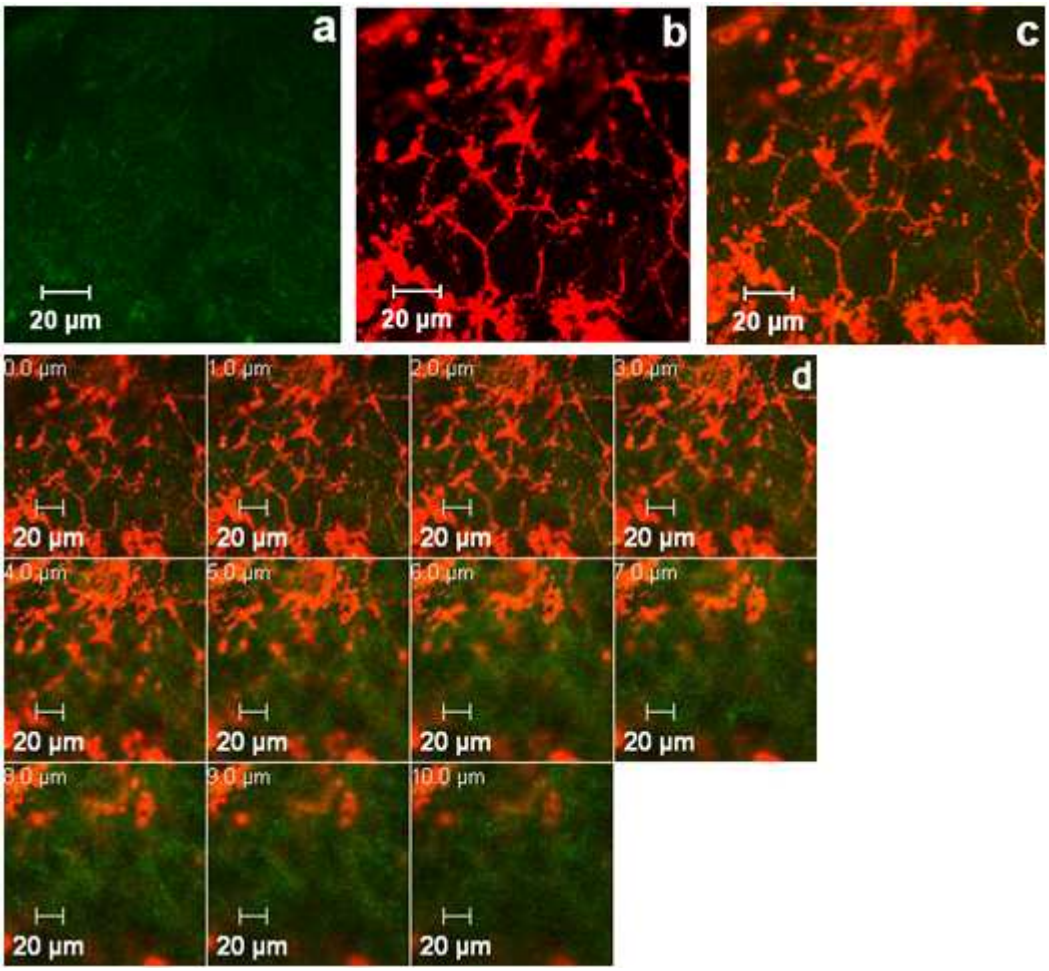

Figure 6. LSCM images (×63) from skin treated with fluorescently-labelled polystyrene NP (31 nm diameter) containing the model active. At the end of a 6-hour application, the skin surface was cleaned thoroughly with buffer and then dried. Panel a shows an almost complete absence of fluorescent NP at the surface suggesting that residual formulations had been effectively removed by washing. In contrast, panel b shows that NR had been released from the NP and had entered the lipid-rich intercellular space between the corneocytes. The overlay (panel c) and the 1 µm optical sections down to 10 µm (panel d) confirm the uptake of "active" into the deeper SC; the weak autofluorescence of the skin itself becomes progressively apparent in the later sections.

The results from the polymethylmethacrylate NP, when the skin surface is properly cleaned at the end of the application period, are similar. Figure 7a shows that no residual fluorescence from the NP is visible on the skin. On the other hand, NR has been released from the NP and has remained on/within the SC post-cleaning (Figure 7b and overlay Figure 7c). Only on hair follicles were the

NP incompletely removed by skin washing (Figure 7d), and co-localization with the "active" was apparent (Figures 7e and 7f).

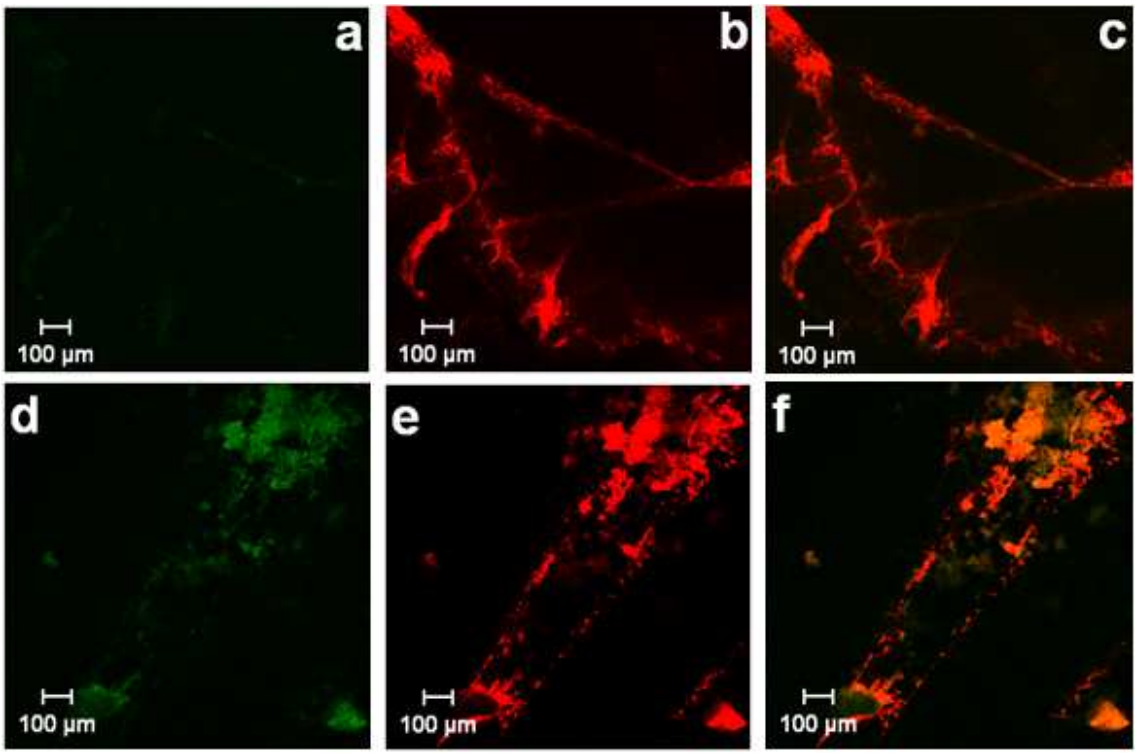

Figure 7. LSCM images from skin treated with fluorescently-labelled polymethylmethacrylate NP (69 nm diameter) containing NR. After a 6-hour application, the skin was thoroughly cleaned with buffer and dried. Panel a shows no residual presence of NP post-washing, while panel b (and overlay panel c) indicates that NR was released from the NP on/into the SC. Only on hair follicles were NP retained after cleaning (panel d) and co-localization of NR on these appendages was observed (panel e and overlay panel f).

Discussion

The confocal images presented in Figures 4 - 7 allow the following, principal conclusions to be drawn: (a) NP made of polystyrene or polymethylmethacrylate do not appear able to pass beyond the most superficial layers of the SC following a topical application lasting 6 hours; (b) the NP show affinity for sequestration in skin furrows and on and around follicles; thorough cleaning can remove the former but not necessarily the latter; (c) the associated hydrophobic active (NR) is

released from the NP and is able to diffuse into the deeper layers of the SC, from which it is not removed by surface cleaning.

The lack of penetration of NP across intact SC is perhaps not too surprising. It is difficult to envisage how a NP might traverse the SC transcellularly (which would involve uptake into corneocytes and translocalization through these cells). Equally, transport in the intercellular channels (100 nm width) of a ~50 nm diameter particle also seems unlikely given that the intercorneocyte space is filled with multiple lipid bilayers. It is also observed in our study that ~30 nm polystyrene nanoparticles did not penetrate beyond the SC. This observation is in agreement with earlier report in the literature.[14] The rigidity of the NP used in this study further undermines the possibility of their permeation across the barrier, as has been suggested in earlier work comparing the uptake of a lipophilic sunscreen from a nanoemulsion and from rigid NP made of cellulose acetate phthalate.[5] Parenthetically, from a practical standpoint, the fact that NP are retarded at the skin surface may be a distinct advantage for a sunscreen formulation,[15] especially if they are able to create an occlusive film as well, from which the active may be slowly released over a prolonged period.[16]

The issue of particle rigidity has also been addressed by comparing standard lipid-based vesicles with specially-designed elastic species.[17, 18] While the penetration of such elastic vesicles across the entire SC has not been equivocally demonstrated, evidence for enhanced "active" transport, and even for the presence of intact vesicles in deeper parts of the SC, has been reported.[18]

Certainly, as has been observed here, it is clear that an "active" associated with topically applied NP can be released from the carrier and diffuses into the SC.[4, 19, 20] As reported elsewhere,[3, 6,

[21, 22] the delivery of the "active" will depend upon its physicochemical properties, its interaction with the nano-carrier, the manner of its association with the particle (surface adhesion, encapsulation, or a mixture of the two), as well as the dimensions and properties (hydrophobicity, hydrophilicity, charge, biodegradability) of the NP themselves.

Further work may be anticipated to explore in greater depth the potential of NP formulations to target "actives" to the hair follicles, for example, or to create a homogeneous and substantive surface film from which prolonged and controlled release may be achieved. Equally, while the penetration of NP across intact SC seems unlikely to pose a toxicological concern, the risk associated with contact to a damaged or diseased skin barrier merits considerable additional research.

Acknowledgements

Supported by the European Commission 6th Research and Technological Development Framework Programme (NAPOLEON: NAnostructured waterborne POLymEr films with OutstaNding properties) and a University Research Scholarship for Xiao Wu.

References

1. Miyazaki, S.; Takahashi, A.; Kubo, W.; Bachynsky, J.; Loebenberg, R. Poly N-Butylcyanoacrylate (PNBCA) Nanocapsules as a Carrier for NSAIDs: In Vitro Release and in Vivo Skin Penetration. *J. Pharm. Pharmaceut. Sci.* **2003,** 6, 238-245.

2. Luengo, J.; Weiss, B.; Schneider, M.; Ehlers, A.; Stracke, F.; Konig, K.; Kostka, K. H.; Lehr, C. M.; Schaefer, U. F. Influence of Nanoencapsulation on Human Skin Transport of Flufenamic Acid. *Skin Pharmacol. Physiol.* **2006,** 19, 190-197.

3. Lboutounne, H.; Chaulet, J. F.; Ploton, C.; Falson, F.; Pirot, F. Sustained Ex Vivo Skin Antiseptic Activity of Chlorhexidine in Poly(ε-Caprolactone) Nanocapsule Encapsulated Form and as a Digluconate. *J. Controlled Release* **2002,** 82, 319-334.

4. Alvarez-Roman, R.; Barre, G.; Guy, R. H.; Fessi, H. Biodegradable Polymer Nanocapsules Containing a Sunscreen Agent: Preparation and Photoprotection. *Eur. J. Pharm. Biopharm.* **2001,** 52, 191-195.

5. Olvera-Martinez, B. I.; Cazares-Delgadillo, J.; Calderilla-Fajardo, S. B.; Villalobos-Garcia, R.; Ganem-Quintanar, A.; Quintanar-Guerrero, D. Preparation of Polymeric Nanocapsules Containing Octyl Methoxycinnamate by the Emulsification-Diffusion Technique: Penetration across the Stratum Corneum. *J. Pharm. Sci.* **2005,** 94, 1552-1559.

6. Luppi, B.; Cerchiara, T.; Bigucci, F.; Basile, R.; Zecchi, V. Polymeric Nanoparticles Composed of Fatty Acids and Polyvinylalcohol for Topical Application of Sunscreens. *J. Pharm. Pharmacol.* **2004,** 56, 407-411.

7. Oberdorster, G.; Oberdorster, E.; Oberdorster, J. Nanotoxicology: An Emerging Discipline Evolving from Studies of Ultrafine Particles. *Environ. Health Perspect.* **2005,** 113, 823-839.

8. Oberdorster, G.; Maynard, A.; Donaldson, K.; Castranova, V.; Fitzpatrick, J.; Ausman, K.; Carter, J.;

Karn, B.; Kreyling, W.; Lai, D.; Olin, S.; Monteiro-Riviere, N.; Warheit, D.; Yang, H. Principles for Characterizing the Potential Human Health Effects from Exposure to Nanomaterials: Elements of a Screening Strategy. *Part. Fibre Toxicol.* **2005,** 2, 8.

9. Borm, P. J.; Robbins, D.; Haubold, S.; Kuhlbusch, T.; Fissan, H.; Donaldson, K.; Schins, R.; Stone, V.; Kreyling, W.; Lademann, J.; Krutmann, J.; Warheit, D.; Oberdorster, E. The Potential Risks of Nanomaterials: A Review Carried out for Ecetoc. *Part. Fibre Toxicol.* **2006,** 3, 11.

10. Hoet, P. H.; Bruske-Hohlfeld, I.; Salata, O. V. Nanoparticles - Known and Unknown Health Risks. *J. Nanobiotechnology* **2004,** 2, 12.

11. Sekkat, N.; Kalia, Y. N.; Guy, R. H. Biophysical Study of Porcine Ear Skin in Vitro and Its Comparison to Human Skin in Vivo. *J. Pharm. Sci.* **2002,** 91, 2376-2381.

12. Simon, G. A.; Maibach, H. I. The Pig as an Experimental Animal Model of Percutaneous Permeation in Man: Qualitative and Quantitative Observations--an Overview. *Skin Pharmacol. Appl. Skin Physiol.* **2000,** 13, 229-234.

13. Lombardi Borgia, S.; Regehly, M.; Sivaramakrishnan, R.; Mehnert, W.; Korting, H. C.; Danker, K.; Roder, B.; Kramer, K. D.; Schafer-Korting, M. Lipid Nanoparticles for Skin Penetration Enhancement-Correlation to Drug Localization within the Particle Matrix as Determined by Fluorescence and Parelectric Spectroscopy. *J. Controlled Release* **2005,** 110, 151-163.

14. Alvarez-Roman, R.; Naik, A.; Kalia, Y. N.; Guy, R. H.; Fessi, H. Skin Penetration and Distribution of Polymeric Nanoparticles. *J. Controlled Release* **2004,** 99, 53-62.

15. Nohynek, G. J.; Lademann, J.; Ribaud, C.; Roberts, M. S. Grey Goo on the Skin? Nanotechnology, Cosmetic and Sunscreen Safety. *Crit. Rev. Toxicol.* **2007,** 37, 251-277.

16. Magdassi, S. Delivery Systems in Cosmetics. *Colloids Surf., A: Physicochem. Eng. Aspects* **1997,** 123-124, 671-679.

17. van den Bergh, B. A.; Vroom, J.; Gerritsen, H.; Junginger, H. E.; Bouwstra, J. A. Interactions of Elastic and Rigid Vesicles with Human Skin in Vitro: Electron Microscopy and Two-Photon Excitation Microscopy. *Biochim. Biophys. Acta* **1999,** 1461, 155-173.

18. Honeywell-Nguyen, P. L.; Gooris, G. S.; Bouwstra, J. A. Quantitative Assessment of the Transport of Elastic and Rigid Vesicle Components and a Model Drug from These Vesicle Formulations into Human Skin in Vivo. *J. Invest. Dermatol.* **2004,** 123, 902-910.

19. Muller, B.; Kreuter, J. Enhanced Transport of Nanoparticle Associated Drugs through Natural and Artificial Membranes--a General Phenomenon? *Int. J. Pharm.* **1999,** 178, 23-32.

20. De Campos, A. M.; Sanchez, A.; Alonso, M. J. Chitosan Nanoparticles: A New Vehicle for the Improvement of the Delivery of Drugs to the Ocular Surface. Application to Cyclosporin A. *Int. J. Pharm.* **2001,** 224, 159-168.

21. Rolland, A.; Wagner, N.; Chatelus, A.; Shroot, B.; Schaefer, H. Site-Specific Drug Delivery to Pilosebaceous Structures Using Polymeric Microspheres. *Pharm. Res.* **1993,** 10, 1738-1744.

22. Calvo, P.; Remuñán-López, C.; Vila-Jato, J. L.; Alonso, M. J. Development of Positively Charged Colloidal Drug Carriers: Chitosan-Coated Polyester Nanocapsules and Submicron-Emulsions. *Colloid Polym. Sci.* **1997,** 275, 46-53.

Glossary of Abbreviations

DLS: dynamic light scattering

FMA: fluorescein methacrylate

KPS: potassium persulfate

LSCM: laser scanning confocal microscope

MMA: methyl methacrylate

NMR: nuclear magnetic resonance

NP: nanoparticle(s)

NR: Nile Red

PI: polydispersity index

PMMA: polymethylmethacrylate

PS: polystyrene

SC: stratum corneum

SDS: sodium dodecylsulphate

TEM: transmission electron microscope

Legends to Table, Chart, Scheme and Figures

Table 1. Properties of the PS and PMMA nanoparticulate (NP) formulations examined[a]

Chart 1. Chemical structures of fluorescein methacrylate (FMA) and Nile Red (NR).

Scheme 1. Polymerization of styrene (Reaction A) and methyl methacrylate (MMA) (Reaction B) with fluorescein methacrylate (FMA) using potassium persulfate (KPS) as an initiator at 75℃.

Figure 1. Transmission electron micrograph of PS and PMMA nanoparticles stained with ruthenium tetroxide (a, b and c, scale bar = 50 nm) or phosphotungstic acid (d, e, and f, scale bar = 200 nm). (a) polystyrene NP alone, (b) polystyrene with fluorescein methacrylate (FMA) polymerized, (c) polystyrene with FMA polymerized and Nile Red (NR) absorbed, (d) polymethylmethacrylate (PMMA) NP alone, (e) PMMA with FMA polymerized, and (f) PMMA with FMA polymerized and NR absorbed.

Figure 2. ^{1}H NMR spectra for (a) PS, FMA and PS-FMA copolymer, and (b) PMMA, FMA and PMMA-FMA copolymer, together with the structures and chemical shift assignments of (c) PS, and (d) PMMA.

Figure 3. LSCM images of the skin surface following a 6-hour application of PS (panels a, b, c) or PMMA nanoparticles (panels d, e, f). In panels a and d, the NP were not fluorescently labelled with

FMA and only a weak green fluorescence from the skin itself is seen. In panels b and e, the NP were fluorescently tagged and the skin surface was not cleaned before imaging; bright green fluorescence is apparent in the skin furrows and around the hair follicles. In panels c and f, the skin surface was cleaned before the confocal images were obtained; only the residual autofluorescence from the skin is observed, suggesting that the NP had been effectively removed by the cleaning procedure.

Figure 4. LSCM images (×10) from skin treated with fluorescently-labelled polystyrene NP (31 nm diameter) containing the model active NR. Panels a and b show fluorescence emission from the skin surface from the NP (panel a) and NR (panel b), respectively. Panel c shows the overlay of panels a and b and the co-localization of NP and "active" at the skin surface. Panels d and e illustrate cross-sectional images, respectively highlighting fluorescence from the NP and from NR. A distinctly labelled, short, trimmed hair is visible. Panel f is the overlay of panels d and e and suggests some permeation of released NR to the deeper skin layers.

Figure 5. LSCM images (×10) from skin treated with fluorescently labelled polymethylmethacrylate NP (69 nm diameter) containing the model active NR. Panels a and b show fluorescence emission from the skin surface from the NP (panel a) and NR (panel b), respectively. Panel c shows the overlay of panels a and b, the presence of NP in the skin furrows and the release of NR from the NP at the skin surface. Panels d and e illustrate cross-sectional images, respectively highlighting fluorescence from the NP and from NR. Another short hair stub is visibly labelled. Panel f is the overlay of panels d and e and again reveals some degree of separation between NP and NR.

Figure 6. LSCM images (×63) from skin treated with fluorescently-labelled polystyrene NP (31 nm diameter) containing the model active. At the end of a 6-hour application, the skin surface was cleaned thoroughly with buffer and then dried. Panel a shows an almost complete absence of fluorescent NP at the surface suggesting that residual formulations had been effectively removed by washing. In contrast, panel b shows that NR had been released from the NP and had entered the lipid-rich intercellular space between the corneocytes. The overlay (panel c) and the 1 µm optical sections down to 10 µm (panel d) confirm the uptake of "active" into the deeper SC; the weak autofluorescence of the skin itself becomes progressively apparent in the later sections.

Figure 7. LSCM images from skin treated with fluorescently-labelled polymethylmethacrylate NP (69 nm diameter) containing NR. After a 6-hour application, the skin was thoroughly cleaned with buffer and dried. Panel a shows no residual presence of NP post-washing, while panel b (and overlay panel c) indicates that NR was released from the NP on/into the SC. Only on hair follicles were NP retained after cleaning (panel d) and co-localization of NR on these appendages was observed (panel e and overlay panel f).